Scalar Dark Matter in the Radio-Frequency Band: Atomic-Spectroscopy Search Results

D. Antypas, O. Tretiak, and A. Garcon
Helmholtz-Institut Mainz, Johannes Gutenberg-Universität Mainz, Mainz 55128, Germany

R. Ozeri
Department of Physics of Complex Systems, Weizmann Institute of Science, Rehovot, Israel 7610001

G. Perez
Department of Particle Physics and Astrophysics, Weizmann Institute of Science, Rehovot, Israel 7610001

D. Budker
Helmholtz-Institut Mainz, Johannes Gutenberg-Universität Mainz, Mainz 55128, Germany
and Department of Physics, University of California at Berkeley, Berkeley, California 94720-300, USA

(Received 12 May 2019; revised manuscript received 2 August 2019; published 3 October 2019)

Among the prominent candidates for dark matter are bosonic fields with small scalar couplings to the standard-model particles. Several techniques are employed to search for such couplings, and the current best constraints are derived from tests of gravity or atomic probes. In experiments employing atoms, observables would arise from expected dark-matter-induced oscillations in the fundamental constants of nature. These studies are primarily sensitive to underlying particle masses below 10^{-14} eV. We present a method to search for fast oscillations of fundamental constants using atomic spectroscopy in cesium vapor. We demonstrate sensitivity to scalar interactions of dark matter associated with a particle mass in the range 8×10^{-11} to 4×10^{-7} eV. In this range our experiment yields constraints on such interactions, which within the framework of an astronomical-size dark matter structure are comparable with, or better than, those provided by experiments probing deviations from the law of gravity.

DOI: 10.1103/PhysRevLett.123.141102

Introduction.—The fundamental constants (FCs) of nature are invariant in time within the standard model (SM) of particle physics, but become dynamical in a number of theories beyond the SM. This possibility has motivated diverse studies that constrain both present-day FC drifts and changes of FCs between the present time and an earlier time in the Universe (see, for example, Refs. [1,2], and references therein).

The FCs are expected to oscillate in cases where the SM fields couple to an ultralight scalar field, coherently oscillating to account for the observed dark matter (DM) density. Within this class of models, FC oscillations are expected to occur at the Compton frequency of the DM particle, $\omega_C = m_\phi$ [3], where m_ϕ is the particle's mass. Such a scenario is particularly motivated in two main cases: (i) where the DM candidate is a dilaton, and its coupling to the SM particles is dictated by scale invariance [4,5], and (ii) the DM is the relaxion field [6], dynamically misaligned from its local minima [7], and its coupling to the SM fields arises due to its mixing with the Higgs boson[8]. Relaxions may form gravitationally bound objects [9], thereby increasing the local DM density and enhancing the observability of the scenario.

There are several proposed schemes to probe light DM that has scalar couplings to SM matter. These include suggestions to look for variations of the fine-structure constant α using atomic clocks [4,10–13], as well as variations in the length of solid objects [10,11,14,15] which would arise from oscillations in α or the electron mass m_e. Direct detection of light scalar DM by probing a DM-induced equivalence-principle- (EP) violating force has also been suggested [16,17]. Existing limits on scalar DM-SM matter interactions come from astrophysical considerations [18] as well as tabletop experiments including radio-frequency (rf) spectroscopy in atomic Dy [19–21], long-term comparison of Cs and Rb clocks [20,22], a network of atomic clocks [23], EP, and fifth-force (FF) experiments [24–27]. In an ongoing experiment [28], a comparison of a Sr atomic clock with a Si cavity [11] is employed to probe scalar DM couplings at frequencies up to 10 Hz, while in Ref. [29] a similar scheme involving spectroscopy with a single Sr^+ ion was used to probe the 1 Hz–1 MHz region (mass range 4×10^{-15}–4×10^{-9} eV).

The most stringent bounds to date on scalar DM-SM matter couplings are the result of searches with atomic probes in the regime below the hertz level, or tests of gravity in EP and FF apparatus. The latter experiments provide constraints up to a frequency of $\sim 10^9$ Hz. Here we present an atomic spectroscopy method for detection of rapid variations of α and m_e that extends the frequency range probed well into the rf band, up to 100 MHz. The rf band is already accessible by EP or FF searches indirectly. Direct probing of fast FC variations with atoms, however, offers a conceptually different approach to studying scalar DM in the particular regime. As we will see, the rf regime is especially interesting for searches for FC oscillations associated with the presence of astronomical-size DM objects.

Our method involves a search for oscillations in the energy spacing ΔE between two electronic levels in atomic ^{133}Cs, the ground state $6s^2S_{1/2}$ and excited state $6p^2P_{3/2}$, while the corresponding transition is resonantly excited with continuous-wave laser light of frequency $f_L \approx f_{\rm atom}$, where $f_{\rm atom} \equiv \Delta E/2\pi$. As this level spacing is approximately proportional [30] to the Rydberg constant $\propto m_e\alpha^2$ [31,32], our scheme is sensitive to oscillations of m_e and α.

In the presence of a light scalar DM field ϕ, α and m_e acquire an oscillatory component, induced by the oscillations of the field at the Compton frequency of the DM particle. On timescales shorter than its coherence time, this field can be expressed as [7]

$$\phi(\vec{r},t) \approx \frac{\sqrt{2\rho_{\rm DM}}}{m_\phi}\sin(m_\phi t), \qquad (1)$$

where $\rho_{\rm DM} \approx 0.4$ GeV/cm^3 is the local DM density [33]. The quantities α and m_e follow the oscillations of ϕ and can be written as

$$\alpha(\vec{r},t) = \alpha_0[1 + g_\gamma\phi(\vec{r},t)], \qquad (2)$$

$$m_e(\vec{r},t) = m_{e,0}\left(1 + \frac{g_e}{m_{e,0}}\phi(\vec{r},t)\right), \qquad (3)$$

where g_γ, g_e are coupling constants of DM to the photon and the electron, respectively. These are assumed independent for a generic DM candidate, but are related within the relaxion DM scenario [7]. If α and m_e oscillate, the resulting fractional change in $f_{\rm atom}$ has amplitude

$$\frac{\delta f_{\rm atom}}{f_{\rm atom}} = 2\frac{\delta\alpha}{\alpha_0} + \frac{\delta m_e}{m_{e,0}} = \left(2g_\gamma + \frac{g_e}{m_{e,0}}\right)\frac{\sqrt{2\rho_{\rm DM}}}{m_\phi}. \qquad (4)$$

When atoms are resonantly excited with light of stable frequency f_L ($f_L \approx f_{\rm atom}$) and in the absence of extraneous noise sources, an observed modulation in the atomic frequency $f_{\rm atom}$ is assumed to arise due to variations of α and m_e. In the absence of detection of such modulation, constraints can be placed on g_γ and g_e. As the detected response of atoms to oscillations in $f_{\rm atom}$ decreases at frequencies greater than the lifetime $\tau = 1/\Gamma$ of the excited state, where $\Gamma = 2\pi \times 5.2$ MHz is the natural linewidth of the $6p^2P_{3/2}$ state, the measured fractional change in $f_{\rm atom}$ has the form

$$\left(\frac{\delta f_{\rm atom}}{f_{\rm atom}}\right)_{\rm meas} = \left(2g_\gamma + \frac{g_e}{m_{e,0}}\right)\frac{\sqrt{2\rho_{\rm DM}}}{m_\phi}\left[1 + \left(\frac{2\pi f}{\Gamma}\right)^2\right]^{-1/2}. \qquad (5)$$

The last term in Eq. (5) is the atomic response function $h_{\rm atom}(f)$, which is ≈ 1 for f, which is below the cutoff $f_{\rm cutoff2} = \Gamma/2\pi$, and it rolls off as $1/f$ for frequencies above $f_{\rm cutoff2}$.

The assumption of stable frequency f_L in its comparison with $f_{\rm atom}$ requires some discussion. If α and m_e oscillate, so does the length L_r of the laser resonator, since it is a multiple of the Bohr radius $1/\alpha m_e$ [10,34], leading to a modulation in f_L. This modulation depends on a different combination of $\delta\alpha/\alpha_0$ and $\delta m_e/m_{e,0}$, compared to that of Eq. (4), and can occur at frequencies as large as $f_{\rm cutoff1} = v_s/L_r \approx 50$ kHz, where $L_r \approx 0.12$ m is the linear dimension of the resonator and $v_s \approx 6000$ m/s is the speed of sound in the stainless-steel-made resonator structure. At frequencies below $f_{\rm cutoff1}$, the induced fractional oscillation in f_L has amplitude [34]

$$\frac{\delta f_L}{f_L} = \frac{\delta\alpha}{\alpha_0} + \frac{\delta m_e}{m_{e,0}} = \left(g_\gamma + \frac{g_e}{m_{e,0}}\right)\frac{\sqrt{2\rho_{\rm DM}}}{m_\phi}. \qquad (6)$$

Comparison of f_L and $f_{\rm atom}$ in the range below $f_{\rm cutoff1}$ therefore offers reduced sensitivity in changes of α, while it is not sensitive to changes of m_e. The measured fractional variation in $f_{\rm atom}$ in this case has amplitude

$$\left(\frac{\delta f_{\rm atom}}{f_{\rm atom}}\right)_{\rm meas} = \frac{\delta\alpha}{\alpha_0} = g_\gamma\frac{\sqrt{2\rho_{\rm DM}}}{m_\phi}, \qquad (7)$$

with $h_{\rm atom}(f) = 1$ here, since $f_{\rm cutoff1} \ll f_{\rm cutoff2}$. In interpreting measurements that check for rapid variations of $f_{\rm atom}$, one has to treat the frequency regimes below and above the cutoff $f_{\rm cutoff1}$ differently. Equation (7) is valid below $f_{\rm cutoff1}$, while Eq. (5) is valid above it [35].

Experiment.—To search for fast variations in the Cs $6S_{1/2} \to 6P_{3/2}$ transition frequency, we employ polarization spectroscopy in a vapor cell [36] [see Fig. 1(a)]. The 7-cm-long cell is placed inside a four-layer magnetic shield and maintained at room temperature. Two counterpropagating laser beams, termed pump and probe, are overlapped inside the cell. The circularly polarized pump induces birefringence in the Cs vapor. Analysis of the polarization of the linearly polarized probe with a balanced polarimeter yields a dispersive-shape feature against laser frequency, for each of the hyperfine components of the transition. These features have narrow widths, nearly limited by the ≈ 5.2 MHz natural linewidth of the transition, and serve as calibrated frequency discriminators. A typical polarization-spectroscopy signal is shown in Fig. 1(b). Fast changes in $f_{\rm atom}$ will appear as amplitude oscillation in the polarimeter output. The quality factor of this oscillation is related to the

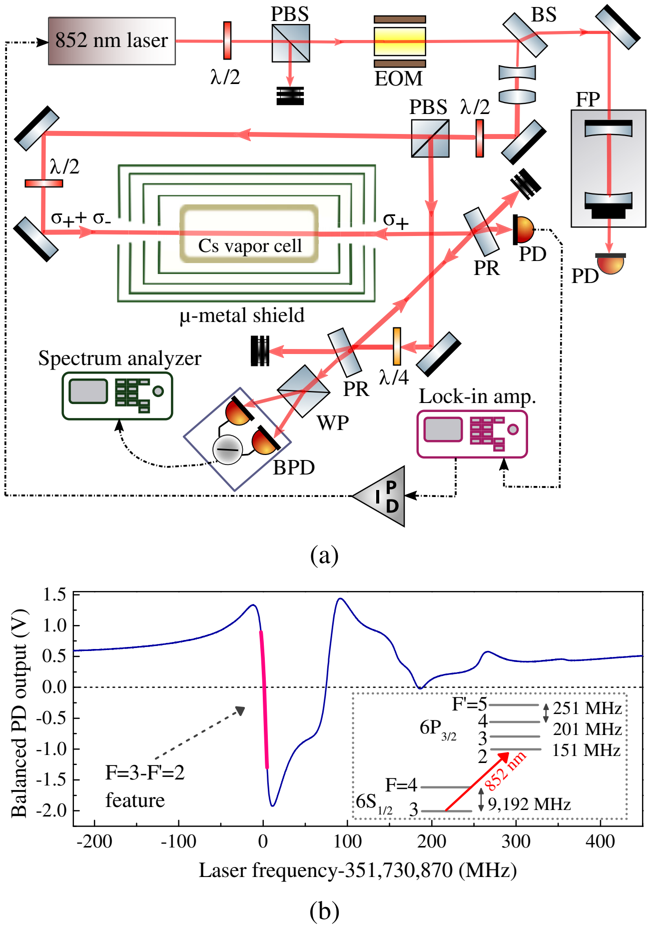

FIG. 1. (a) Experimental apparatus. (P)BS, (polarizing) beam splitter; FP, Fabry-Perot interferometer; EOM, electro-optic modulator; (B)PD, (balanced) photodetector; WP, Wollaston prism; PR, partial reflector. $\lambda/2$, half-wave plate; $\lambda/4$, quarter-wave plate. (b) Polarization spectroscopy on the $6S_{1/2}F = 3 \rightarrow 6P_{3/2}F' = 2, 3, 4$ transitions. The pink line indicates the feature employed for frequency discrimination. Inset shows the hyperfine structure of ground $6S_{1/2}$ state and excited $6P_{3/2}$ state.

coherence of the field ϕ of Eq. (1) and is given by $\omega/\Delta\omega \approx 2\pi/v_{\rm DM}^2 \approx 6\times10^6$, where $v_{\rm DM} = 10^{-3}$ is the virial velocity of the DM field [37]. (In the case of a relaxion halo, a longer coherence time is expected, resulting in a larger quality factor [9].) Within the 20 kHz–100 MHz band probed in the experiment, the expected spectral width $\Delta\omega/2\pi$ of the oscillation is in the range 3 mHz–17 Hz.

To account for the decrease in the atomic response at frequencies above the transition linewidth, and other response nonuniformities in the apparatus, a frequency calibration is required. This is done by imposing frequency modulation on the laser light with the use of an electro-optic modulator (EOM), and comparing the amplitudes of this modulation, as measured with the atoms and with a Fabry-Perot cavity of known characteristics that serves as a calibration reference.

During an experiment, the laser frequency is tuned to excite atoms from the $F = 3$ hyperfine level of the ground state to the $F' = 2$ level of the excited state. The output of the balanced polarimeter is measured with a spectrum analyzer (Keysight N9320B). The calibration of this analyzer for measurements of absolute power of magnitude similar to that detected in the actual experiment (~2 fW/Hz) was checked by measurement of a signal of known power spectral density. To produce a high-resolution noise-power spectrum in the 20 kHz–100 MHz range, measurements in ≈22 000 frequency windows are required, each of which consists of 461 bins; a bin is 10 Hz wide and corresponds to integration time of 5 ms. Approximately 22 hours is required to acquire such a spectrum. To ensure long-term frequency stability of the laser, its frequency is stabilized to the atomic resonance. This is achieved by modulating f_L at 167 Hz with an amplitude of 200 kHz, and demodulation of the measured probe beam power with a lock-in amplifier provides an error signal, to which the laser frequency is stabilized with a bandwidth of 2 Hz.

Data analysis.—A set of three high-resolution noise-power spectra in the 20 kHz-100 MHz range were acquired and analyzed to probe fast oscillations in $f_{\rm atom}$. The mean and variance of each spectrum were computed in several selected frequency regions and were found to be consistent among the three spectra to within 2%. The slope of the $F = 3 \rightarrow F' = 2$ feature in the polarization spectrum of Fig. 1(b), relevant to the sensitivity in detecting oscillations in $f_{\rm atom}$, was stable to within 6% during the entire 66-h-long acquisition run. An averaged spectrum was computed from the three high-resolution power spectra. The sensitivity in detection of FC oscillations at a given frequency is related to the fluctuations of the noise-power level in that spectrum, within the particular frequency range (see analysis in Ref. [38]). For each frequency bin within this range, the noise fluctuations define a global threshold (i.e., accounting for the look elsewhere effect) at the 95% confidence level [39]. Any peak above this threshold must be then investigated for possible detection. A number of such peaks were present in the averaged spectrum. These were checked using methods described in Ref. [38]. No signal of unknown origin with power above the threshold was detected. In its absence, an upper limit is placed on possible oscillations of the frequency $f_{\rm atom}$, which is presented in Fig. 2 at the 95% C.L.

Constraints on scalar DM couplings.—We use the obtained bounds on $\delta f_{\rm atom}/f_{\rm atom}$ to constrain the parameters g_γ and g_e of Eqs. (2) and (3). With the assumption that DM-induced oscillations in f_a arise solely due to either the coupling to the photon or to the electron, we set bounds on the corresponding coupling constants, and present these in Figs. 3(a) and 3(b). In the same plots, corresponding limits derived from analysis [17] of results of EP experiments, as well as limits derived from naturalness, are also shown. In the case of a scalar field ϕ, naturalness requires that

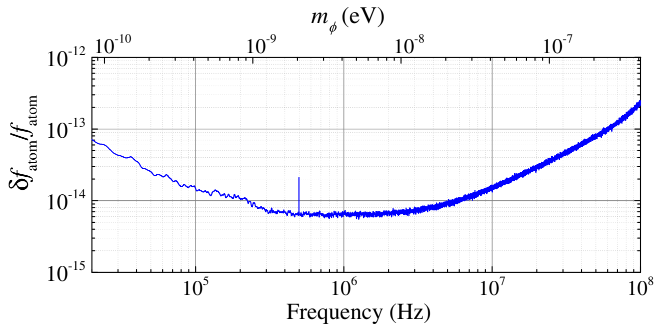

FIG. 2. Upper bounds on the fractional modulation $\delta f_{\rm atom}/f_{\rm atom}$, shown at the 95% C.L. The reduced sensitivity in the range 498330 ± 5 Hz is due to increased apparatus noise. At frequencies below 300 kHz the sensitivity is limited by technical noise of the laser, and above 5 MHz by the decaying response of the atoms. In the range 300 kHz–5 MHz, the sensitivity is nearly limited by the shot noise of the probe light that is measured with the balanced polarimeter shown in Fig. 1(a) [38].

radiative corrections to the mass m_ϕ, arising due to its interactions, be smaller than the mass itself [14,16]. In the present work, where a DM field that has scalar couplings to SM matter is considered, this requirement leads to the constraints $|g_e| < 4\pi m_\phi/\Lambda$, $|g_\gamma| < 16\pi m_\phi/\Lambda^2$, where Λ is the cutoff scale for the Higgs mass [7].

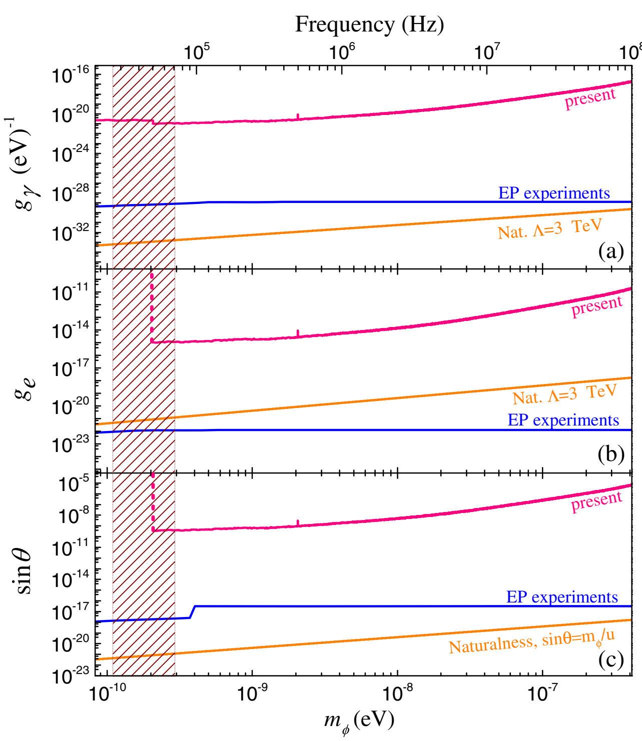

FIG. 3. Constraints on scalar DM parameters at the 95% C.L., obtained with use of the limits on $\delta f_{\rm atom}/f_{\rm atom}$ shown in Fig. 2. The bounds derived from EP experiments are from Ref. [17]. Constraints from the requirement for naturalness are explained in the text. The shaded area centered around the cutoff frequency of 50 kHz $[(1-3)\times 10^{-10}$ eV] indicates a region in which careful modeling of the laser resonator response is required to determine the transition in sensitivity to the various parameters constrained.

To obtain the bounds of Figs. 3(a) and 3(b), g_γ and g_e were treated independently. Within the relaxion DM model [7], however, this assumption is not valid. These couplings are related; both acquire values dependent on the relaxion-Higgs mixing, which is parametrized in terms of a mixing angle θ. For the range of mass m_ϕ probed in this work (10^{-10}–10^{-6} eV), the contribution of the relaxion coupling to the electron is expected to dominate the oscillations in f_a [7]. One can therefore assume that $\delta f_{\rm atom}/f_{\rm atom} \approx \delta m_e/m_e$ in Eq. (4) and employ the defining relation between g_e and the mixing angle θ, to constrain θ within the investigated m_ϕ region. The parameter g_e is given by [7]

$$g_e = Y_e \sin\theta, \tag{8}$$

where Y_e is the Higgs-electron Yukawa coupling, for which the accepted value within the SM is $Y_e \approx 2.9\times 10^{-6}$ [40]. We show the obtained bounds on $\sin\theta$ in Fig. 3(c), along with corresponding bounds placed from EP experiments, and by the requirement to maintain naturalness. Within the relaxion DM framework, this requirement results in the constraint $\sin\theta \le m_\phi/v$ [41], where $v = 246$ GeV is the Higgs vacuum expectation value.

An enhancement in the amplitude of FC oscillations is expected in the presence of an astronomical-scale DM object around Earth or in its vicinity. Such an enhancement would occur due to an increase in the local DM density $\rho_{\rm DM}$ [see Eqs. (1)–(3)]. Searches for transient variations of α using a network of GPS satellites [42] and a terrestrial network of remotely located atomic clocks [23] have provided constraints on topological DM. Here we consider the scenario of an Earth-bound relaxion halo, examined in Ref. [9]. We make use of the computed DM density $\rho_{\rm DM}$ [9] at the surface of Earth to provide more stringent constraints on the couplings g_γ and g_e than those shown in Fig. 3 (conditional on the existence of the relaxion halo). These tighter bounds are presented in Fig. 4. In the presence of the halo, the enhancement in $\rho_{\rm DM}$ is expected to be mostly pronounced in the mass range 10^{-12}–10^{-8} eV. We note that the corresponding frequency regime 10^4–10^8 Hz has been out of reach for most of the laboratory searches for variations of FC, which, with the exception of the recent work [29], have been mostly sensitive to frequencies below 1 Hz.

Discussion and outlook.—The obtained constraints on light DM scalar interactions with SM matter extend the frequency range investigated with atomic probes to 10^8 Hz, a regime not previously searched directly. More stringent bounds on the scalar coupling to the photon and the electron exist within the 20 kHz–100 MHz range of this work. Such constraints, however, are derived from EP and

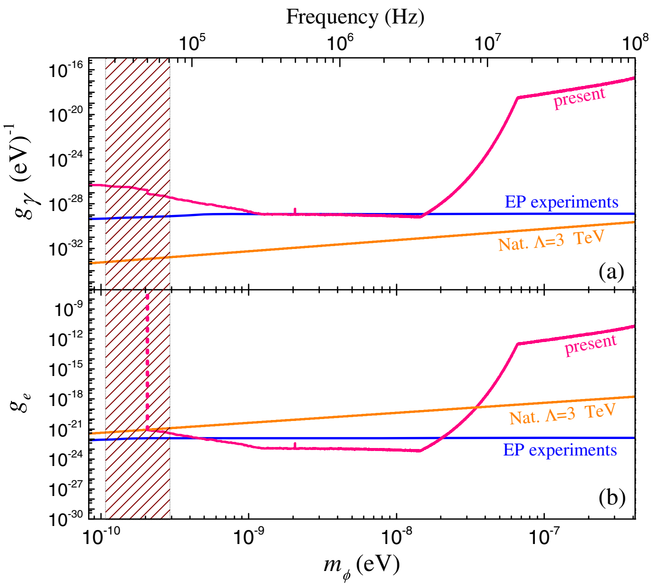

FIG. 4. Bounds on the parameters g_γ, g_e with consideration to a relaxion halo gravitationally bound by Earth. The DM density assumed within this scenario is computed in Ref. [9]. The shaded area is the same as that in Fig. 3.

FF experiments, which are not directly sensitive to rapid oscillations of FC, as is the method demonstrated here.

The sensitivity in detection of DM-induced FC variations for given bounds on $\delta f_{\text{atom}}/f_{\text{atom}}$ is inversely proportional to the frequency (mass) probed [see Eq. (4)]. Use of atomic clocks is therefore advantageous, in that these probes typically search the subhertz regime, with resulting DM constraints competing against those provided by EP and FF studies. Without assuming any enhancement in the local DM density due to Earth, our polarization spectroscopy scheme is unlikely to approach a sensitivity level comparable to that offered by EP or FF searches because of the higher frequencies being probed. However, searching for rapid FC oscillations in the rf band allows us to access a frequency range, which as discussed might provide enhanced sensitivity in detection of FC variations within scenarios of an Earth-bound DM halo. As seen in Fig. 4, the bounds from polarization spectroscopy are at regions better than those set by EP results. Improvements in detection of modulation in the Cs energy levels involved in the experiment would enable a search deeper into the parameter space of g_γ and g_e.

Several apparatus upgrades are under way. The primary improvement involves a change in the scheme employed to obtain the frequency spectrum of the polarization-spectroscopy signal. The spectrum analyzer currently used will be replaced with fast data-acquisition electronics with the ability to perform real-time high-resolution spectral analysis, thereby increasing the effective integration time drastically. An optimization of the signal-to-noise ratio in the polarization spectroscopy setup is also being explored. These improvements, combined with a longer integration time of up to $\sim 10^4$ h, should result in a sensitivity enhancement in excess of 10^3. This level of improvement is sufficient to explore scalar interactions between DM and SM matter with a sensitivity better than that of other methods in a significant fraction of the parameter space accessible by polarization spectroscopy.

We are grateful to M. G. Kozlov, V. V. Flambaum, V. Dzuba, and Y. Stadnik for fruitful discussions. We acknowledge technical support from A. Brogna, M. Schott, T. H. Lin, and A. Düdder. The work is supported by the European Research Council (ERC) under the European Union's Horizon 2020 research and innovation programme (Dark-OST, Grant Agreement No. 695405), and the DFG Reinhart Koselleck project. The work of G. P. is supported by grants from the BSF, ERC, ISF; the work of R. O. and G. P. is jointly supported by the Minerva Foundation, and the Segre Research Award. The work of R. O. is supported by the ISF, ERC, and the Israeli Ministry of Science and Technology.

[1] M. S. Safronova, D. Budker, D. DeMille, D. F. Jackson Kimball, A. Derevianko, and C. W. Clark, Rev. Mod. Phys. **90**, 025008 (2018).
[2] J. P. Uzan, C.R. Phys. **16**, 576 (2015).
[3] We use natural units, where $\hbar = c = 1$.
[4] A. Arvanitaki, J. Huang, and K. Van Tilburg, Phys. Rev. D **91**, 015015 (2015).
[5] P. W. Graham, I. G. Irastorza, S. K. Lamoreaux, A. Lindner, and K. A. Van Bibber, Annu. Rev. Nucl. Part. Sci. **65**, 485 (2015).
[6] P. W. Graham, D. E. Kaplan, and S. Rajendran, Phys. Rev. Lett. **115**, 221801 (2015).
[7] A. Banerjee, H. Kim, and G. Perez, arXiv:1810.01889.
[8] T. Flacke, C. Frugiuele, E. Fuchs, R. S. Gupta, and G. Perez, J. High Energy Phys. 06 (2017) 50.
[9] A. Banerjee, D. Budker, J. Eby, H. Kim, and G. Perez, arXiv:1902.08212.
[10] Y. V. Stadnik and V. V. Flambaum, Phys. Rev. Lett. **114**, 161301 (2015).
[11] Y. V. Stadnik and V. V. Flambaum, Phys. Rev. A **93**, 063630 (2016).
[12] M. S. Safronova, S. G. Porsev, C. Sanner, and J. Ye, Phys. Rev. Lett. **120**, 173001 (2018).
[13] E. Savalle, B. M. Roberts, F. Frank, P.-E. Pottie, B. T. McAllister, C. B. Dailey, A. Derevianko, and P. Wolf, arXiv:1902.07192.
[14] A. Arvanitaki, S. Dimopoulos, and K. Van Tilburg, Phys. Rev. Lett. **116**, 031102 (2016).
[15] A. A. Geraci, C. Bradley, D. Gao, J. Weinstein, and A. Derevianko, Phys. Rev. Lett. **123**, 031304 (2019).
[16] P. W. Graham, D. E. Kaplan, J. Mardon, S. Rajendran, and W. A. Terrano, Phys. Rev. D **93**, 075029 (2016).
[17] A. Hees, O. Minazzoli, E. Savalle, Y. V. Stadnik, and P. Wolf, Phys. Rev. D **98**, 064051 (2018).
[18] Y. V. Stadnik and V. V. Flambaum, Phys. Rev. Lett. **115**, 201301 (2015).
[19] K. Van Tilburg, N. Leefer, L. Bougas, and D. Budker, Phys. Rev. Lett. **115**, 011802 (2015).

[20] Y. V. Stadnik and V. V. Flambaum, Phys. Rev. A **94**, 022111 (2016).
[21] N. Leefer, A. Gerhardus, D. Budker, V. V. Flambaum, and Y. V. Stadnik, Phys. Rev. Lett. **117**, 271601 (2016).
[22] A. Hees, J. Guéna, M. Abgrall, S. Bize, and P. Wolf, Phys. Rev. Lett. **117**, 061301 (2016).
[23] P. Wcisło *et al.*, Sci. Adv. **4**, eaau4869 (2018).
[24] P. Touboul *et al.*, Phys. Rev. Lett. **119**, 231101 (2017).
[25] J. Bergé, P. Brax, G. Métris, M. Pernot-Borràs, P. Touboul, and J. P. Uzan, Phys. Rev. Lett. **120**, 141101 (2018).
[26] E. G. Adelberger, J. H. Gundlach, B. R. Heckel, S. Hoedl, and S. Schlamminger, Prog. Part. Nucl. Phys. **62**, 102 (2009).
[27] T. A. Wagner, S. Schlamminger, J. H. Gundlach, and E. G. Adelberger, Classical Quantum Gravity **29**, 184002 (2012).
[28] C. Kennedy, E. Oelker, T. Bothwell, D. Kedar, L. Sonderhouse, E. Marti, S. Bromley, J. Robinson, and J. Ye, *49th Annual Meeting of the APS Division of Atomic, Molecular and Optical Physics APS Meeting* (2018), Vol. 63, http://meetings.aps.org/Meeting/DAMOP18/Session/H06.5.
[29] S. Aharony, N. Akerman, R. Ozeri, G. Perez, I. Savoray, and R. Shaniv, arXiv:1902.02788.
[30] The dependence $\Delta E \propto m_e \alpha^2$ is accurate to within relativistic corrections of order $(\alpha Z)^2 \approx 16\%$ in Cs.
[31] V. A. Dzuba, V. V. Flambaum, and J. K. Webb, Phys. Rev. Lett. **82**, 888 (1999).
[32] V. A. Dzuba, V. V. Flambaum, and J. K. Webb, Phys. Rev. A **59**, 230 (1999).
[33] R. Catena and P. Ullio, J. Cosmol. Astropart. Phys. 08 (2010) 004.
[34] M. G. Kozlov and D. Budker, Ann. Phys. **531**, 1800254 (2018).
[35] The frequency f_L of the laser is referenced to the resonance frequency of an internal optical cavity, with a stabilization bandwidth of ≈5 kHz. The experiment, however, is carried out at frequencies in the range 20 kHz–100 MHz, which are higher than this additional cutoff. Therefore, the effects of FC-induced oscillations in f_L arising due to the internal cavity need not be considered.
[36] W. Demtröder, *Laser Spectroscopy 2*, 5th ed. (Springer, Berlin-Heidelberg, 2015).
[37] L. Krauss, J. Moody, F. Wilczek, and D. Morris, Phys. Rev. Lett. **55**, 1797 (1985).
[38] See Supplemental Material at http://link.aps.org/supplemental/10.1103/PhysRevLett.123.141102 for details on analysis of raw data and apparatus sensitivity.
[39] J. D. Scargle, Astrophys. J. **263**, 835 (1982).
[40] W. Altmannshofer, J. Brod, and M. Schmaltz, J. High Energy Phys. 05 (2015) 125.
[41] C. Frugiuele, E. Fuchs, G. Perez, and M. Schlaffer, J. High Energy Phys. 10 (2018) 151.
[42] B. M. Roberts, G. Blewitt, C. Dailey, M. Murphy, M. Pospelov, A. Rollings, J. Sherman, W. Williams, and A. Derevianko, Nat. Commun. **8**, 1195 (2017).